Entropy Analysis of Mixed Convective Magnetohydrodynamic Flow of a Viscoelastic Fluid over a Stretching Sheet

Adnan S. Butt[a], Sufian Munawar[a], Asif Ali[a], and Ahmer Mehmood[b]

[a] Department of Mathematics, Quaid-I-Azam University 45320, Islamabad 44000, Pakistan
[b] Department of Mathematics, FBAS, International Islamic University, Islamabad 44000, Pakistan

Reprint requests to A. S. B.; E-mail: adnansaeedbutt85@gmail.com

Z. Naturforsch. **67a,** 451 – 459 (2012) / DOI: 10.5560/ZNA.2012-0055
Received October 28, 2012 / revised March 27, 2012

In the present article, an investigation is made on entropy generated within a mixed convective magnetohydrodynamic flow of a viscoelastic fluid over a stretching sheet. In performing the analysis, it is assumed that the flow is steady, laminar, and fully developed. The governing equations for velocity and temperature fields are transformed into nonlinear ordinary differential equations by using suitable similarity transformations and are solved using the homotopy analysis method. The expressions for local entropy generation number Ns, average entropy $[\mathrm{Ns}]_{\mathrm{avg}}$, Bejan number Be, and average Bejan number $[\mathrm{Be}]_{\mathrm{avg}}$ are obtained using the corresponding velocity and temperature data. A comprehensive parametric study is presented through graphs.

Key words: Boundary Layer Flow; Viscoelastic Fluid; Mixed Convection; Entropy Generation; Homotopy Analysis Method.

1. Introduction

The study of boundary layer flows over a stretching sheet have attracted considerable attention during the last few decades due to its wide applications in many industrial and manufacturing processes such as petroleum drilling, extrusion processes, manufacturing of foods and paper, cooling of metallic plates, and many other similar activities. An extensive study has been made by scientists and researcher in both theoretical and industrial contexts. Crane [1] first studied the laminar boundary layer flow of a Newtionian fluid caused by the stretching of an elastic flat sheet having a velocity varying linearly with distance from a fixed point due to application of a unifrom stress. Thereafter, numerous investigations were made on the stretching sheet problem with linear stretching [2 – 6]. All the aforementioned studies are restricted to Newtonian fluids. However in the recent years, it has been observed that most of the industrial processes such as molten plastics, artificial fibres, polymeric liquid, blood, food stuff exhibit non-Newtonian fluid behaviour. For this reason, a fundamental analysis of momentum and thermal boundary layer flows of non-Newtonian fluids adjacent to a stretching sheet is an important issue in the areas of fluid dynamics and heat transfer.

The study of viscoelastic fluids has gained importance in the last few years. Rajagopal et al. [7] investigated the boundary layer flow for a class of viscoelastic fluids known as second-grade fluids over a stretching sheet. Chang [8] showed the non-uniqueness of the solution for the viscoelastic fluid flow over a stretching sheet. Dandapat and Gupta [9] and Vajravelu and Rollins [10] studied the flow and heat transfer characteristics of a viscoelastic fluid over a stretching sheet. Idrees and Abel [11] analyzed the heat transfer in a viscoelastic fluid past a stretching surface in a porous medium with internal heat generation. Cortell [12] discussed the flow and heat transfer of a viscoelastic fluid over a stretching surface considering both constant sheet temperature and prescribed sheet temperature.

In recent years, numerous investigations have been conducted on the magnetohydrodynamic (MHD) flows because of its important applications in metallurgical industry such as cooling of continous strips etc. Andersson [13] examined the flow of a viscoelastic fluid over a stretching surface under the influence of a uniform magetic flield and showed that the magnetic parameter has the same effect as that of the viscoelastic parame-

ter in flow characteristics. Vajravelu and Rollins [14] examined the hydromagnetic flow in an electrically conducting second-grade fluid over a stretching sheet. Seddeek [15] studied the heat and mass transfer of a viscoelastic fluid over a stretching sheet through a porous medium in the presence of a transverse magnetic field and internal heat source or sink.

In all the papers cited earlier, the effects of buoyancy forces were neglected. However in many practical situations the buoyancy forces arising due to heating or cooling of the continuous stretching surfaces alter the flow and thermal fields. Shenoy and Mashelkar [16] discussed the laminar natural convection heat transfer in a viscoelastic fluid. Ali and Al-Yousef [17] studied the laminar mixed convection from a continuously moving vertical surface with suction or injection. Hsiao [18] examined the heat and mass transfer in an electrically conducting mixed convective viscoelastic fluid with radiation effects.

Although the preceeding research works have discussed a lot about fluid flow and heat transfer in Newtonian and non-Newtonian fluids, they have been restricted to only first-law analysis from thermodynamical point of view. In thermodynamical analysis of flow and heat transfer processes, one thing of core interest is to improve the thermal systems to avoid the energy losses and fully utilize the energy resources. Second-law analysis in terms of entropy generation rate is a useful tool for predicting the performance of the engineering processes by investigating the irreversibility arising during the processes. Different sources such as heat transfer and viscous dissipation are responsible for the generation of entropy [19, 20]. Entropy generation in flow systems was investigated by Bejan [21]. He showed that engineering design of a thermal system could be improved through minimizing the entropy generation. Sahin [22] introduced the second-law analysis to a viscous fluid in circular duct with isothermal boundary conditions. Yilbas et al. [23] studied entropy generation in a semi-blocked pipe including swirling effect. Arikoglu et al. [24] analyzed the effects of on entropy generation in magnetohydrodynamic flow over a rotating disk by using a semi-numerical analytical solution technique known as differential transform method (DTM). The influence of viscous dissipation on entropy gneration due to natural convection from a heated horizontal isothermal cylinder in oil was investigated by Abu-Hijleh et al. [25]. Mahmud and Fraser [26, 27] applied the second-law analysis to fundamental convective heat transfer problems and to non-Newtonian fluid flow through a channel made of two parallel plates. Odat et al. [28] studied the effect of magnetic field on entropy generation due to laminar forced convection past a horizontal flat plate. Aiboud and Saouli [29] analyzed the effect of entropy generation for viscoelastic magnetohydrodynamic flow over a stretching surface and observed that the viscoelastic parameter has a slight effect on entropy production.

The purpose of the present article is to study the entropy production in a mixed convective magnetohydrodynamic flow of a viscoelastic fluid over a stretching sheet and to identify the parameters which are responsible for the augmention of entropy production and the losses of energy. Suitable similarity transformations are used to transform the fundamental equations of hydrodynamic and thermal boundary layer flow into ordinary differential equations which are then solved by the homotopy analysis method. The expressions for local entropy generation number Ns, average entropy $[\mathrm{Ns}]_{\mathrm{avg}}$, Bejan number Be, and average Bejan number $[\mathrm{Be}]_{\mathrm{avg}}$ are presented and the results are discussed graphically and quantitatively.

2. Mathematical Formulation of the Problem

Consider a steady state, laminar, two-dimensional mixed convective flow of a viscoelastic fluid past a flat stretching surface in the presence of a uniform transverse magnetic field. The stretching surface is coinciding with the plane $y = 0$ and the flow being confined to $y > 0$. The origin is kept fixed while the wall is stretching and the y-axis is perpendicular to the surface. The continous stretching surface is assumed to have linear velocity. Also it is assumed that the fluid is electrically conducting and the magnetic Reynolds number is small so that the induced magnetic field is neglected. No electic field is assumed to exist, and the stretching surface is assumed to be electrically insulating. An incompressible, homogenous, second-grade fluid having a constitutive equation based on the postulate of gradually fading memory suggested by Rivlin and Ericksen [30] is being used for the present problem. The Cauchy stress tensor $\mathbf{T}$ of second grade has the form

$$\mathbf{T} = -p\mathbf{I} + \mu\mathbf{A}_1 + \alpha_1\mathbf{A}_2 + \alpha_2\mathbf{A}_1^2, \tag{1}$$

where p is the pressure, $\mathbf{I}$ the unit tensor, and μ the dynamic viscosity. α_1 and α_2 are the first and the second

normal stress cofficients that are related to the material modulus and for the present second-grade fluid

$$\mu \geq 0, \quad \alpha_1 \geq 0, \quad \alpha_1 + \alpha_2 = 0. \tag{2}$$

The Kinematic tensors $\mathbf{A}_1$ and $\mathbf{A}_2$ are defined as

$$\mathbf{A}_1 = \nabla \mathbf{V} + (\nabla \mathbf{V})^{\mathrm{T}}, \tag{3}$$

$$\mathbf{A}_2 = \frac{\mathrm{d}\mathbf{A}_1}{\mathrm{d}t} + \mathbf{A}_1(\nabla \mathbf{V}) + (\nabla \mathbf{V})^{\mathrm{T}}\mathbf{A}_1, \tag{4}$$

where $\mathbf{V}$ is the velocity and $\frac{\mathrm{d}}{\mathrm{d}t}$ the material derivative. The steady two-dimensional boundary-layer equations for this flow, heat transfer in usual notations, are given by

$$\frac{\partial u}{\partial x} + \frac{\partial v}{\partial y} = 0, \tag{5}$$

$$u\frac{\partial u}{\partial x} + v\frac{\partial u}{\partial y} = \nu\frac{\partial^2 u}{\partial y^2} + \frac{\alpha_1}{\rho}\left[\frac{\partial}{\partial x}\left(u\frac{\partial^2 u}{\partial y^2}\right) + \frac{\partial u}{\partial y}\frac{\partial^2 v}{\partial y^2} + v\frac{\partial^3 u}{\partial y^3}\right] + g\beta(T - T_\infty) - \frac{\sigma B_0^2 u}{\rho}, \tag{6}$$

$$u\frac{\partial T}{\partial x} + v\frac{\partial T}{\partial y} = \frac{k}{\rho c_{\mathrm{p}}}\frac{\partial^2 T}{\partial y^2} + \frac{\alpha_1}{\rho c_{\mathrm{p}}}\left[u\frac{\partial u}{\partial y}\frac{\partial^2 u}{\partial x \partial y} + v\frac{\partial u}{\partial y}\frac{\partial^2 u}{\partial y^2}\right]. \tag{7}$$

The well-known Boussinesq approximation is used to represent the buoyancy mixed term. Here u and v are the velocity components in the x- and y-directions, α_1 is the material constant, T the temperature, g the magnitude of the gravity, ν the kinematic viscosity, β the coefficient of thermal expansion, T_∞ the temperature of the ambient fluid, ρ the density, c_{p} the specific heat at constant pressure, k the thermal conductivity, σ the electrical conductivity, and B_0 the magnetic field parameter, respectively. The boundary conditions to the problem are

$$u = u_{\mathrm{w}} = ax, \quad v = 0 \quad \text{at} \quad y = 0, \quad a > 0, \tag{8}$$

$$u \to 0 \quad \text{at} \quad y \to \infty,$$

$$T = T_{\mathrm{w}} \quad \text{at} \quad y = 0, \tag{9}$$

$$T = T_\infty \quad \text{at} \quad y \to \infty,$$

where T_{w} and T_∞ are constant wall temperature and ambient fluid temperature, a and A are the proportional constants, and L is the characteristic length.

Introducing the similarity transformations

$$u = axf'(\eta), \quad v = -(a\nu)^{\frac{1}{2}} f(\eta), \quad \eta = (a/\nu)^{\frac{1}{2}} y. \tag{10}$$

Substituting (10) into (6), we have

$$f'^2 - ff'' = f''' + K(2f'f''' - f''^2 - ff^{IV}) + \lambda\theta - Mf', \tag{11}$$

where $K = \alpha_1 a/\rho\nu$ is the viscoelastic parameter, $\lambda = \frac{Gr}{\mathrm{Re}^2} = \frac{g\beta(T_{\mathrm{w}} - T_\infty)/a^2 x}{u_{\mathrm{w}}^2 x^2/\nu^2}$ is the mixed convection parameter, and $M = \sigma B_0^2/\rho a$ is the magnetic parameter. The corresponding boundary conditions become

$$f = 0, \quad f' = 1 \quad \text{at } \eta = 0, \quad f' \to 0 \quad \text{at } \eta \to \infty. \tag{12}$$

For the prescribed surface temperature, we introduce the dimensionless temperature $\theta(\eta)$:

$$\theta(\eta) = \frac{T - T_\infty}{T_{\mathrm{w}} - T_\infty}. \tag{13}$$

Using (10) and (13), (7) and the boundary conditions (9) can be written as

$$\theta'' + \mathrm{Pr} f\theta' + \mathrm{PrEc}[f''^2 + K(f'f''^2 - ff''f''')] = 0 \tag{14}$$

with the boundary conditions

$$\theta = 1 \quad \text{at} \quad \eta = 0, \quad \theta \to 0 \quad \text{at} \quad \eta \to \infty, \tag{15}$$

where $\mathrm{Pr} = \mu c_{\mathrm{p}}/k$ is the Prandtl number and $\mathrm{Ec} = a^2x^2/c_{\mathrm{p}}(T_{\mathrm{w}} - T_\infty)$ is the Eckerd number.

2.1. Entropy Generation

The volumetric rate of local entropy generation, in the case of the existence of a magnetic field, can be expressed in the following form [20, 31]:

$$S_{\mathrm{G}} = \frac{k}{T_\infty^2}(\nabla T)^2 + \frac{\mathbf{T} : \nabla \mathbf{V}}{T_\infty} + \frac{1}{T_\infty}[(J - QV)(E + V \times B)], \tag{16}$$

where k is the thermal conductivity, μ the viscosity, T_∞ a reference temperature, J the electric current, Q the electric charge density, V the velocity vector, E the electric field, and B the magnetic induction. It is assumed that J is much greater than QV. Also, the electric force per unit charge E, is assumed to be negligible compared to the magnetic force per unit charge, $V \times B$.

Clearly (16) shows the contribution of three sources of entropy generation. The first term on the right hand side is the local entropy generation due to heat transfer; the second term is the local entropy generation due to fluid friction, whereas the third term is due to the effects of magnetic field. Equation (16) can be further simplified for the present problem as follows:

$$S_{\mathrm{G}} = \frac{k}{T_\infty^2}\left(\frac{\partial T}{\partial y}\right)^2 + \frac{1}{T_\infty}\left[\mu\left(\frac{\partial u}{\partial y}\right)^2 + \alpha_1 u\frac{\partial u}{\partial y}\frac{\partial^2 u}{\partial x \partial y} + \alpha_1 v\frac{\partial u}{\partial y}\frac{\partial^2 u}{\partial y^2}\right] + \frac{\sigma B_0^2}{T_\infty}u^2 . \tag{17}$$

It is appropriate to define a dimensionless number for the entropy generation rate Ns as

$$\mathrm{Ns} = \frac{S_{\mathrm{G}}}{S_{\mathrm{G0}}} = \mathrm{Re}_L\theta'^2 + \mathrm{Re}_L\frac{\mathrm{Br}}{\Omega}f''^2 + \frac{\mathrm{Br}}{\Omega}\mathrm{Re}_L K(f'f''^2 - ff''f''') + \frac{\mathrm{Br}}{\Omega}\mathrm{Re}_L M f'^2 , \tag{18}$$

where $S_{\mathrm{G0}} = \frac{k(T_{\mathrm{w}}-T_\infty)}{T_\infty^2 L^2}$ is the characteristic entropy generation rate, $\Omega = \frac{T_\infty}{T_{\mathrm{w}}-T_\infty}$ is the dimensionless temperature difference, $\mathrm{Re}_L = \frac{u_L L}{\nu}$ is the Reynolds number, and $\mathrm{Br} = \mathrm{Pr}\,\mathrm{Ec}$ is the Brinkman number, respectively. Thus the dimensionless form of local entropy generation in (18) can be expressed as

$$\mathrm{Ns} = N_H + N_{\mathrm{f}} + N_m = N_H + N_F , \tag{19}$$

where N_H is the local entropy generation due to heat transfer, N_{f} the local entropy generation due to fluid friction, and N_m the local entropy generation due to joule dissipation. During calculation it may be possible to evaluate these terms separately, then compare them to see the dominance of one term on the other. The averaged entropy generation number can be evaluated using the following integral formula:

$$[Ns]_{\mathrm{avg}} = \frac{1}{\forall}\int_{\forall} Ns\,\mathrm{d}\forall , \tag{20}$$

where $\forall$ is the length of the boundary layer region.

Another alternative irreversibility distribution parameter is the Bejan number Be which is the ratio of entropy generation due to heat transfer to the total entropy generation:

$$\mathrm{Be} = \frac{N_H}{Ns} . \tag{21}$$

From (21), it is very obvious that the value of the Bejan number ranges from 0 to 1. The zero value of the Bejan number corresponds to the limit where the irreversibility is dominated by the combined effects of fluid friction and joule dissipation while $\mathrm{Be} = 1$ is the limit where the irreversibility due to heat transfer dominates the flow system. The contributions of both the factors to entropy generation are equal when the Bejan number is equal to half.

The average Bejan number is given as

$$[\mathrm{Be}]_{\mathrm{avg}} = \frac{1}{\forall}\int_{\forall} \mathrm{Be}\,\mathrm{d}\forall . \tag{22}$$

3. Solution of the Problem

In order to solve equations (11), (12), (14), and (15), we use the analytic technique homotopy analysis method (HAM), a powerful method to solve nonlinear problems. This method was proposed by Liao [32], and in the recent few years, this method has been successfully employed to solve many types of nonlinear problems in science and engineering. Taking into account the boundary conditions (12) and (15), the initial guesses and linear operators can be chossen as

$$f_0(\eta) = 1 - \mathrm{e}^{-\eta}, \quad \theta_0(\eta) = \mathrm{e}^{-\eta} \tag{23}$$

and

$$\mathcal{L}_f = \frac{\mathrm{d}^3 f}{\mathrm{d}\eta^3} - \frac{\mathrm{d}f}{\mathrm{d}\eta} , \tag{24}$$

$$\mathcal{L}_\theta = \frac{\mathrm{d}^2\theta}{\mathrm{d}\eta^2} - \theta . \tag{25}$$

The solutions obtained by HAM are in the forms of series given by

$$f(\eta) = \sum_{m=0}^{\infty} f_m(\eta) , \tag{26}$$

$$\theta(\eta) = \sum_{m=0}^{\infty} \theta_m(\eta) . \tag{27}$$

All the remaining facts of the method are renowned and therefore are concealed here for simplicity (see for instance [33–36]).

3.1. Convergence of HAM Solution

The accuracy and convergence of our approximate solution series (26) and (27) strongly dependent upon the convergence controlling parameters [32], say $\hbar_1$

Order	$-f''(0)$	$-\theta'(0)$
[4/4]	1.196000	0.427366
[8/8]	1.19526	0.427207
[12/12]	1.19526	0.427201
[16/16]	1.19526	0.427201
[20/20]	1.19526	0.427201

Table 1. Covergence table for $-f''(0)$ and $-\theta'(0)$ using $[m,m]$ homtopy padé approximation.

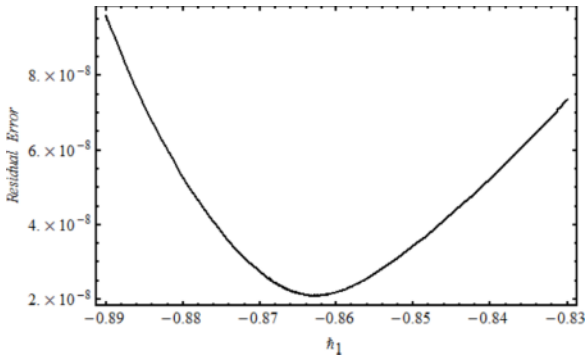

Fig. 1. Residual error of velocity profile at 20th iteration when $M = 1$, $\mathrm{Pr} = 1$, $\mathrm{Ec} = 0.2$, $K = 0.2$, $\lambda = 0.2$.

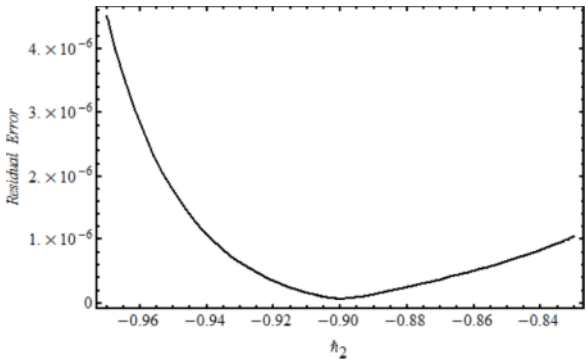

Fig. 2. Residual error of temperature profile at 20th iteration when $M = 1$, $\mathrm{Pr} = 1$, $\mathrm{Ec} = 0.2$, $K = 0.2$, $\lambda = 0.2$.

and $\hbar_2$.The graphs for residual errors and a table showing the convergence of our solution series are given and discussed in this section. To accelerate the rate of convergence of our solutions series (26) and (27), we use the homotopy Padé approximation. From Table 1 it can be observed that after 12th order of approximation it seems that solutions converge up to six decimal places. Figures 1 and 2 illustrate the accuracy of our solution. From Figure 1, it is observed that by fixing other physical parameters the residual error at 20th order of approximation is 2.22548×10^{-8} at $\hbar_1 = -0.843517$. Similarly, for energy equation the residual error at 20th iteration is 7.02501×10^{-8} at $\hbar_2 = -0.911523$. Hence

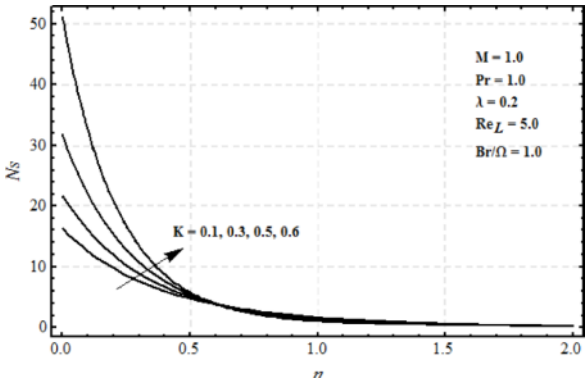

Fig. 3. Effect of viscoelastic parameter on entropy generation number with $M = 1$, $\mathrm{Pr} = 1$, $\mathrm{Re}_L = 5$, $\mathrm{Ec} = 0.2$, $\lambda = 0.2$, $\mathrm{Br}/\Omega = 1$.

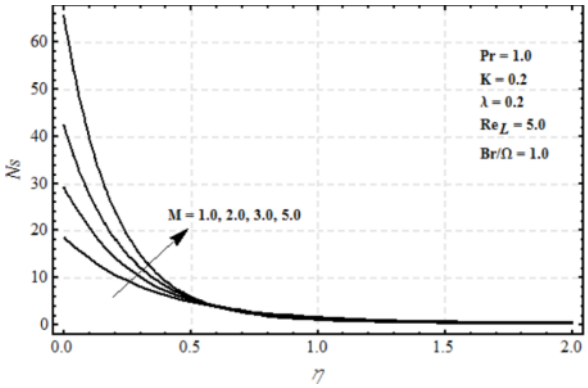

Fig. 4. Effect of magnetic parameter on entropy generation number with $K = 0.2$, $\mathrm{Pr} = 1$, $\mathrm{Re}_L = 5$, $\mathrm{Ec} = 0.2$, $\lambda = 0.2$, $\mathrm{Br}/\Omega = 1$.

Figures 1 and 2 ensure the good accuracy of our solution series.

3.2. Results and Discussions

In this section, we have investigated the effects of different parameters on the entropy generation through graphical illustration to understand physical aspects of the considered problem. The variation in local entropy generation number Ns is shown in Figures 3 – 5 for different values of parameters. In Figure 3, the effects of viscoelastic parameter K on the local entropy generation number is discussed. It is observed that by increasing the viscoelastic parameter K there is an increase in the local entropy generation number. Thus it is noticed that the presence of a viscoelastic fluid is to increase

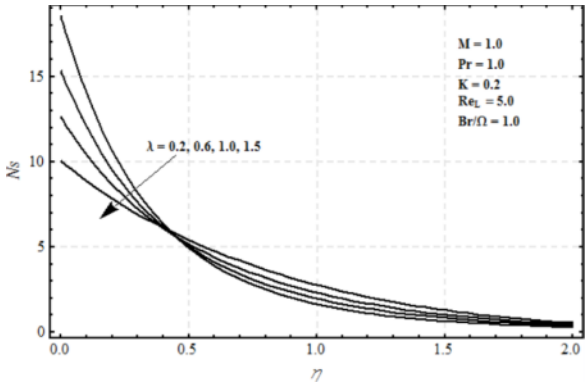

Fig. 5. Effect of λ on entropy generation number with $K = 0.2$, $M = 1$, $\mathrm{Re}_L = 5$, $\mathrm{Pr} = 1$, $\mathrm{Ec} = 0.2$, $\mathrm{Br}/\Omega = 1$.

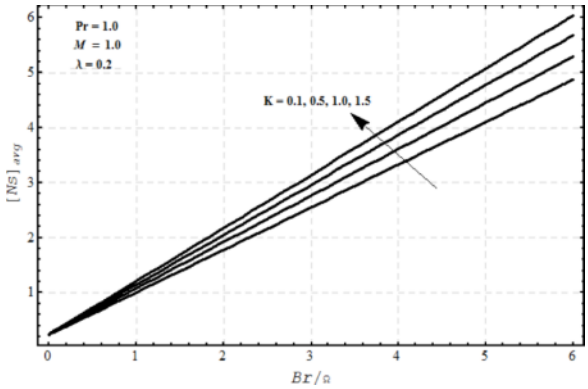

Fig. 6. Effect of viscoelastic parameter on average entropy generation plotted against group parameter with $M = 1$, $\mathrm{Pr} = 1$, $\mathrm{Re}_L = 5$, $\lambda = 0.2$.

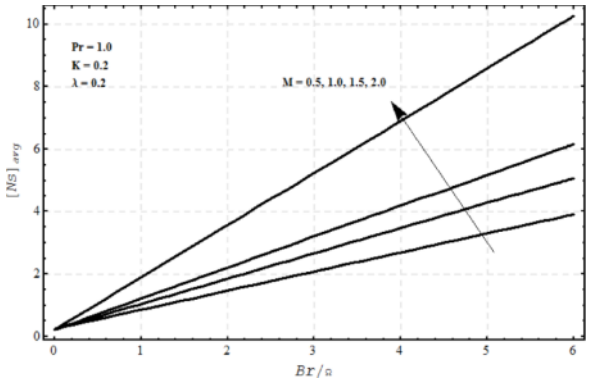

Fig. 7. Effect of magnetic parameter on average entropy generation plotted against group parameter with $K = 0.2$, $\mathrm{Pr} = 1$, $\mathrm{Re}_L = 5$, $\lambda = 0.2$.

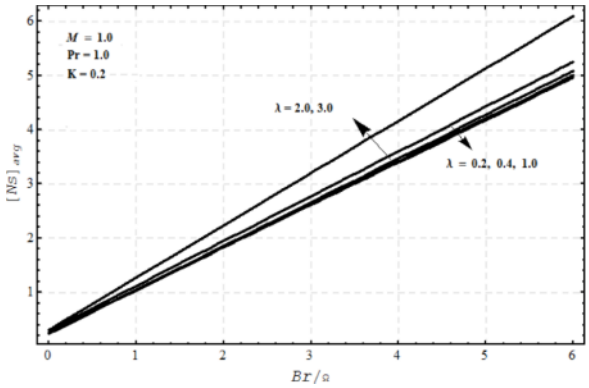

Fig. 8. Effect of mixed convection parameter on average entropy generation plotted against group parameter with $M = 1$, $\mathrm{Pr} = 1$, $K = 0.2$, $\mathrm{Re}_L = 5$.

the entropy production. Figure 4 depicts the effects of the magnetic parameter M on Ns. It is seen from the figure that there is an increase in local entropy generation number with an increase in the magnetic parameter M. The presence of the magnetic field creates more entropy in the fluid. Also it is observed that the entropy production is high at the surface. In Figure 5 it is noticed that with an increase in the mixed convection parameter λ, the local entropy generation number Ns decreases near the surface. However, as one moves away from the surface the effects are reversed. Moreover, in all the cases the entropy generation number is higher near the surface where the temperature and velocity gradients are large. This means that the surface is a strong source of entropy generation.

Figures 6 – 8 show the variation of the averaged entropy generation number $[\mathrm{Ns}]_{\mathrm{avg}}$ against the group parameter Br/Ω for different physical parameters. The reason for choosing the group parameter Br/Ω as the variational parameter is its practical importance and significant contribution in entropy generation. Figure 6 shows that for a particular value of the viscoelastic parameter K it is noticed that the average entropy is an increasing function of Br/Ω. So the irreversibility increases as the group parameter increases. Also there is an increase in average entropy by increasing the value of K. Figure 7 illustrates that the averaged entropy generation increases as the magnetic parameter M increases. Figure 8 depicts that within the range $0 < \lambda < 1$, $[\mathrm{Ns}]_{\mathrm{avg}}$ decreases and for large values of λ, the average entropy increases.

The entropy generation number Ns is good for generating a spatial entropy profile, but fails in giving any idea about which kind of irreversibility contributes

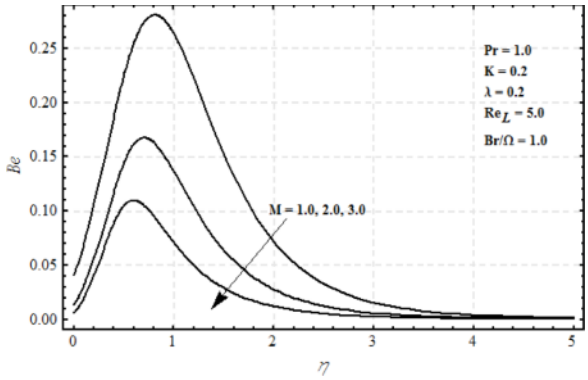

Fig. 9. Effect of magnetic parameter on Bejan number with $K = 0.2$, $\mathrm{Pr} = 1$, $\mathrm{Re}_L = 5$, $\mathrm{Ec} = 0.2$, $\lambda = 0.2$, $\mathrm{Br}/\Omega = 1$.

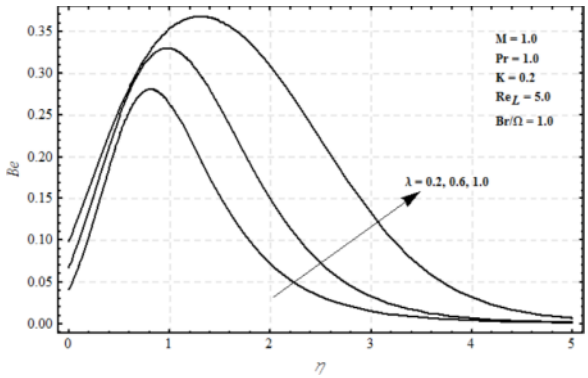

Fig. 10. Effect of mixed convection parameter on Bejan number with $K = 0.2$, $M = 1$, $\mathrm{Re}_L = 5$, $\mathrm{Ec} = 0.2$, $\mathrm{Pr} = 1$, $\mathrm{Br}/\Omega = 1$.

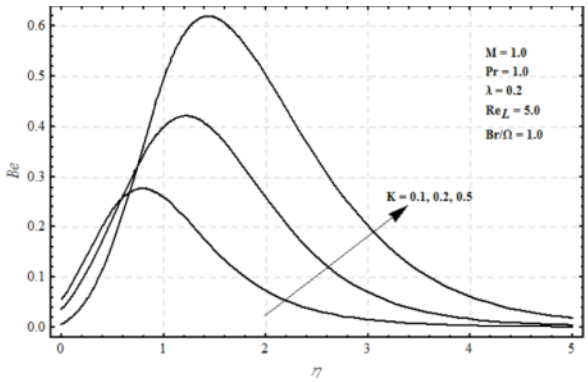

Fig. 11. Effect of viscoelastic parameter on Bejan number with $M = 1$, $\mathrm{Pr} = 1$, $\mathrm{Re}_L = 5$, $\mathrm{Ec} = 0.2$, $\lambda = 0.2$, $\mathrm{Br}/\Omega = 1$.

more. For this purpose, the Bejan number Be is introduced in order to identify whether the heat transfer irreversibility dominates or the fluid friction and the Joule dissipation. In Figures 9 – 11, the effects of different

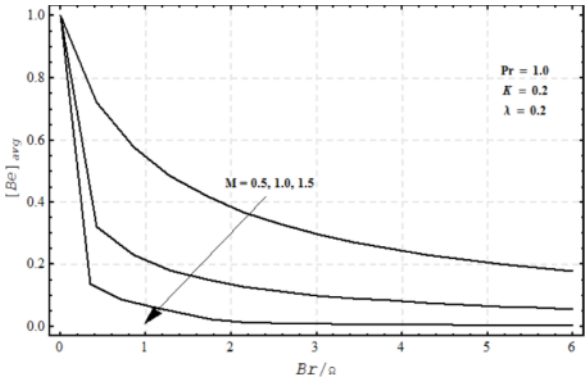

Fig. 12. Effect of magnetic field parameter M on average Bejan number plotted against group parameter with $K = 0.2$, $\mathrm{Pr} = 1$, $\mathrm{Re}_L = 5$, $\mathrm{Ec} = 0.2$, $\lambda = 0.2$.

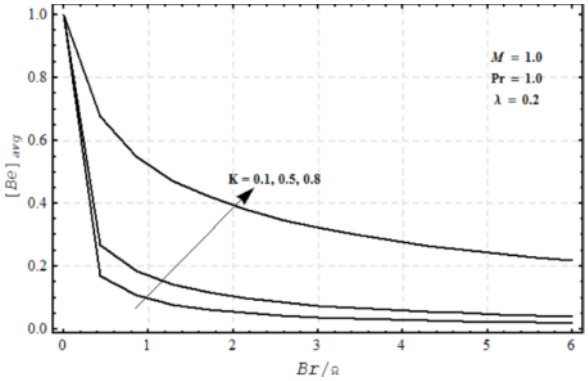

Fig. 13. Effect of viscoelastic parameter K on average Bejan number plotted against group parameter with $M = 1$, $\mathrm{Pr} = 1$, $\mathrm{Re}_L = 5$, $\mathrm{Ec} = 0.2$, $\lambda = 0.2$.

physical parameters on the Bejan number are plotted against η. It is observed that the irreversibility effects due to fluid friction and joule dissipation are dominant at the surface of the stretching sheet. With an increase in distance from the stretching surface, the irreversibility effects due to heat transfer start to appear and attain a peak value within the boundary layer region. From there, a decreasing behaviour is seen and in the free stream region, the irreversibility due to fluid friction and joule dissipation is again dominant. Also it is noteworthy that there is a decrease in the heat transfer irreversibility within the boundary layer with an increase in magnetic parameter M as illustrated in Figure 9. On the otherhand, the heat transfer irreversibility within the boundary layer increases with mixed convection parameter λ and viscoelastic parameter K as shown in Figures 10 and 11.

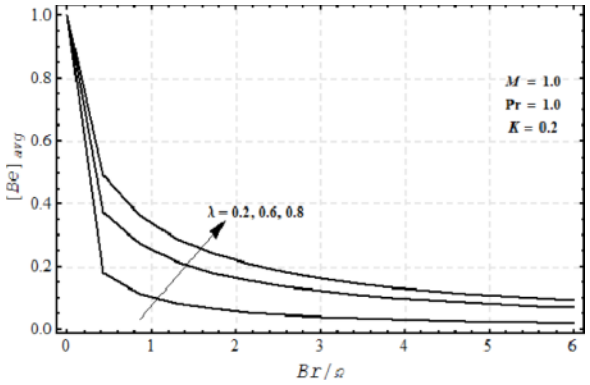

Fig. 14. Effect of mixed convection parameter λ on average Bejan number plotted against group parameter with $M = 1$, $\mathrm{Pr} = 1$, $K = 0.2$, $\mathrm{Re}_L = 5$, $\mathrm{Ec} = 0.2$.

The average Bejan number $[\mathrm{Be}]_{\mathrm{avg}}$ is plotted against the group parameter for different physical parameters in Figures 12 – 14. The influence of magnetic parameter M on the averaged Bejan number is presented in Figure 12. It is observed that for a fixed value of M, the fluid friction and joule dissipation irreversibilities become stronger as the group parameter increases. Also by increasing M, irreversibilities due to fluid friction and joule dissipation become more dominant. On the otherhand, these effects become weak by increasing the viscoelastic parameter K and mixed convection parameter λ as illustrated in Figures 13 and 14.

4. Summary and Conclusions

The boundary layer flow of a magnetohydrodynamic, mixed convective viscoelastic fluid over a stretching surface is studied. The velocity and temperature profiles are used to compute local entropy generation number Ns, average entropy $[\mathrm{Ns}]_{\mathrm{avg}}$, Bejan number Be, and average Bejan number $[\mathrm{Be}]_{\mathrm{avg}}$. The influences of physical parameters involved in the problem on entropy generation number and Bejan number are discussed. It is observed that local entropy generation number Ns and average entropy $[\mathrm{Ns}]_{\mathrm{avg}}$ increases with increase in viscoelastic parameter K and magnetic parameter M. On the otherhand it is observed that there is a decrease in average entropy for mixed convection parameter λ within the range $0 < \lambda < 1$. For $\lambda > 1$, the entropy production rate increases. Thus the engineering devices, such as natural based cooling systems and solar collectors, will operate with a higher efficiency for the mixed convection parameter λ having a value between 0 and 1 due to less irreversibility effects. It is observed that the surface of the stretching sheet is a strong source of irreversibility. The Bejan number shows that the irreversibility due to fluid friction and joule dissipation become dominant with the increase in magnetic parameter M, and with an increase in viscoelastic parameter K and mixed convection parameter λ, the irreversibility effects due to heat transfer start to appear.

The results obtained through this article depict that the effects of entropy generated in the considered system can be reduced by choosing the appropriate values of the physical parameters.

Acknowledgement

We are grateful to the reviewers for expert comments and suggestions for improving this paper.

[1] L. J. Crane, Z. Angew. Math. Phys. **21**, 645 (1970).
[2] W. H. H. Banks, J. Mec. Theor. Appl. **2**, 375 (1983).
[3] C. K. Chen and M. I. Char, J. Math. Anal. Appl. **135**, 568 (1988).
[4] P. S. Gupta and A. S. Gupta, Can J. Chem. Eng. **55**, 744 (1977).
[5] L. J. Grubka and K. M. Bobba, ASME J. Heat Transfer **107**, 248 (1985).
[6] A. Ali and A. Mehmood, Commun. Nonlin. Sci. Numer. Simul. **13**, 340 (2008).
[7] K. R. Rajagopal, T. Y. Na, and A. S. Gupta, Rheo. Acta. **23**, 213 (1984).
[8] W. D. Chang, Q. Appl. Math. **47**, 365 (1989).
[9] B. S. Dandapat and A. S. Gupta, Int. J. Nonlin. Mech. **24**, 215 (1989).
[10] K. Vajravelu and D. Rollins, J. Math. Anal. Appl. **158**, 241 (1991).
[11] M. K. Idrees and M. S. Abel, Indian J. Theor. Phys. **44**, 233 (1996).
[12] R. Cortell, Int. J. Nonlin. Mech. **41**, 78 (2006).
[13] H. I. Andersson, Acta Mech. **95**, 227 (1992).
[14] K. Vajravelu and D. Rollins, Appl. Math. Comput. **148**, 789 (2004).
[15] M. A. Seddeek, Comp. Material Sci. **38**, 781 (2007).
[16] A. V. Shenoy and R. A. Mashelkar, Chem. Eng. Sci. **33**, 769 (1978).

[17] M. Ali and F. Al-Yousef, Heat Mass Transfer **33**, 301 (1998).
[18] K. L. Hsiao, Commun. Nonlin. Sci. Numer. Simul. **15**, 1803 (2010).
[19] A. Bejan, Adv. Heat Transfer **15**, 1 (1982).
[20] A. Bejan, Entropy Generation Minimization, CRC Press, Boca Raton, FL, USA, 1996.
[21] A. Bejan, J. Heat Transfer **101**, 718 (1979).
[22] A. Z. Sahin, J. Heat Transfer **120**, 76 (1998).
[23] B. S. Yilbas, S. Z. Shuja, and M. O. Budair, Int. J. Heat Mass Transfer **42**, 4027 (1999).
[24] A. Arikoglu, I. Ozkol, and G. Komurgoz, Appl. Energy **85**, 1225 (2008).
[25] A. K. Abu-Hijleh, I. N. Jadallah and E. A. Nada, Int. Commun. Heat Mass Transfer **25**, 1135 (1998).
[26] S. Mahmud and R. A. Fraser, Int. J. Therm. Sci. **42**, 177 (2003).
[27] S. Mahmud and R. A. Fraser, Exergy **2**, 140 (2002).
[28] M. Q. A. Odat, R. A. Damseh, and M. A. A. Nimr, Entropy **4**, 293 (2004).
[29] S. Aiboud and S. Saouli, Int. J. Nonlin. Mech. **44**, 482 (2010).
[30] R. S. Rivlin and J. L. Ericksen, J. Rat. Mech. Anal. **4**, 323 (1955).
[31] L. C. Woods, Thermodynamics of Fluid System, Oxford University Press, Oxford, UK 1975.
[32] S. J. Liao, Beyond Perturbation: Introduction to Homotopy Analysis Method. Chapman & Hall/CRC Press, London/Boca Raton 2003.
[33] A. Mehmood, A. Ali, and T. Shah, Canadian J. Phys. **86**, 1079 (2008).
[34] A. Mehmood, S. Munawar, and A. Ali, Commun. Nonlin. Sci. Numer. Simul. **15**, 4233 (2010).
[35] A. Ali and A. Mehmood, ASME J. Heat Transfer **130**, 121701 (2008).
[36] G. Domairry and N. Nadim, Int. Commun. Heat Mass Transfer **35**, 93 2008.